



Title	X-ray absorption spectroscopy studies on the structure and the catalytic activity of nickel phosphide catalysts [an abstract of entire text]
Author(s)	Rashid, Md. Harun Al
Citation	北海道大学. 博士(工学) 甲第14677号
Issue Date	2021-09-24
Doc URL	http://hdl.handle.net/2115/83239
Type	theses (doctoral - abstract of entire text)
Note	この博士論文全文の閲覧方法については、以下のサイトをご参照ください。
Note(URL)	https://www.lib.hokudai.ac.jp/dissertations/copy-guides/
File Information	Md._Harun_AI_Rashid_summary.pdf



[Instructions for use](#)

X-ray absorption spectroscopy studies on the structure and the catalytic activity of nickel phosphide catalysts

Md Harun Al Rashid
Candidate for the Degree of Doctoral
Supervisor: Professor Kiyotaka ASAKURA
Division of Quantum Science and Engineering

Introduction

X-ray absorption fine structure (XAFS) spectroscopy is the most promising technique for the atomic-level characterization of the inorganic-oxide-supported catalysts. It provides us element-specific detailed information on the electronic state and the local structure. As XAFS can characterize local structure accurately even if the long-range order is not present in the sample, we can obtain the electronic and structural information on the powder or the solution samples by XAFS analysis. XAFS is composed of both X-ray Absorption Near Edge Structure (XANES) appearing near X-ray absorption edge and Extended X-ray Absorption Fine Structure (EXAFS) appearing above the edge from 50 eV to 1000 eV. XANES and EXAFS have been widely used in different fields in science like biology, material science, fundamental physics, which are carried out by measuring the x-ray absorption coefficient of a substance as a function of energy.

I have applied the XAFS to determine the SiO₂-supported nickel phosphide (Ni-P) catalysts structures, which have been found to show the high activity for Non-Oxidative Coupling of Methane (NOCM) reaction. The NOCM is now an essential reaction because CH₄ is a good candidate for the alternative feedstock of petroleum to produce organic materials. Ni-P catalytic structures have a strong Ni:P ratio dependence on their activities. Ni-P/SiO₂ (Initial Ni:P = 1:1) shows the most effective conversion of CH₄ to higher hydrocarbons for NOCM, indicating the structure of Ni-P catalysts depends on the Ni:P ratio. However, nickel phosphide compounds have a complex structure, and it is challenging to decide the structure of the Ni-P catalyst exactly.

The main objective of this thesis is to reveal the active structure and make the relation between reaction activity and structure of nickel phosphide catalysts for non-oxidative coupling of methane (NOCM) reaction. To achieve this goal, I investigated the structure of Ni-P/SiO₂ catalysts with different initial Ni:P ratios of 1:1, 2:1, and 3:1 by XAFS. XAFS is the most suitable technique to investigate the local structure of the unknown sample. It provides us qualitative information (valence state and coordination geometry) and quantitative information (bond distance R , coordination number N) around the X-ray absorbing atom from XANES and EXAFS analysis, respectively. However, there are several drawbacks in EXAFS and XANES analysis. I analyze the EXAFS data

using the conventional curve fitting method to achieve the catalytically active structure of SiO₂-supported nickel phosphide among the three samples which have been found highly active for non-oxidative coupling of methane (NOCM) reaction. But the conventional analysis of EXAFS by curve fitting (CF) method has the limitation of parameters by Nyquist theory. This limitation cannot allow me to analyze the data because of the complex nickel phosphide system, which contains many scattering atoms. Even if I reduce the number of fitting parameters, the obtained data were not directly related to a real structure. Due to the lack of references and limitation of parameters, I cannot confirm the structure of the other two structures with Ni and P ratios of 2:1 and 3:1.

On the other hand, XANES gives the electronic state and geometrical symmetry around the X-ray absorbing atom in the complex system straightforwardly. XANES studies require pattern fitting by comparing the reference and unknown as a fingerprint. But the lack of a reference sample hindered our XANES analysis. The recent development of XANES calculations like FEFF enables us to provide a theoretical reference. For the theoretical computation of XANES spectra, the spherical average of atoms, the so-called muffin-tin approximation, is widely adopted for the sake of simplicity of the theory. But muffin-tin approximation cannot properly describe a large number of physical systems such as low dimensional systems and systems having large interstitial space like, e.g., diamond and layered structure. For light elements, atomic potential scattering is rather weak, and thus scattering of the interstitial potential is comparatively strong. Hence full potential (FP) corrections are important. Here, the brand new method has been used for the theoretical XANES calculations called FPMS (full potential multiple scattering). In my doctoral work, I carried out structural analyses of Ni phosphide catalysts on SiO₂ with initial Ni:P ratios of 1:1, 2:1, and 3:1 using theoretical models without the use of experimental reference compounds.

Experimental

The SiO₂-supported Ni phosphide catalysts with initial Ni:P ratios of 1:1, 2:1, and 3:1 were prepared by a conventional impregnation method, followed by temperature-programmed reduction. The catalytic activities were tested at 1173 K using a conventional fixed-bed gas-flow system

(Figure 3-3). The sample was denoted as Ni-P/SiO₂ (Ni:P = X:Y, Z h), where X:Y represents the initial Ni:P molar ratio and Z is the reaction time. Professor Yamanaka and his research group prepared these samples.¹

X-ray absorption fine structure (XAFS) spectra were recorded at the BL9C beamline of the Photon Factory (PF: 2.5 GeV, 450 mA) at the Institute for Materials Structure Science (KEK-IMSS-PF). The X-rays were monochromatized by a Si (111) double crystal and were focused by a Rh-coated bent cylindrical mirror. The higher harmonics were rejected by the mirror. The Ni K-edge data were collected in a transmission mode. The incident and transmitted X-rays were detected by 100% N₂ gas-filled and (15% N₂ and 85% Ar) mixed-gas-filled ionization chambers, respectively. The EXAFS analyses were carried out using the REX2000 software (Rigaku Co).² Fourier transformed range was 3-16 Å⁻¹ for the experimental and theoretical data analysis.

The theoretical XANES and EXAFS spectra were calculated using the FEFF8 code³, which uses self-consistent multiple scattering theory with a muffin-tin potential approximation.⁴ For the exchange-correlation potential, the Hedin-Lundqvist complex potential was used to obtain fine spectra with a typical full-potential multiple scattering (FMS) radius of 5.0 Å for theoretical XANES calculations.

Results and Discussion

Ni K-edge EXAFS spectrum for both fresh and spent samples are compared with reference Ni₂P after background subtraction in Figure 1. The three different Ni:P ratios samples give different EXAFS oscillations. Figure 1(b) shows the EXAFS oscillation of the sample Ni-P/SiO₂ (Ni:P = 1:1), similar to that of the Ni₂P reference, indicating that Ni-P/SiO₂ (Ni:P = 1:1) had the Ni₂P structure. Ni-P/SiO₂ (Ni:P = 2:1) and Ni-P/SiO₂ (Ni:P = 3:1) have quite different oscillations from the Ni₂P reference. This different oscillation is indicating different Ni phosphide phase forms in these two samples.

The Fourier transform of the Ni K-edge EXAFS spectra and the fresh and spent samples have been shown in Figure 2. The Ni-P/SiO₂ (Ni:P = 1:1) showed two distinct peaks in this Fourier transform (Figure 2(b)). The main peak and first peak are corresponding to the Ni-Ni and Ni-P bond distances, respectively. Compared to the reference Ni₂P, the Fourier transform depicted a similar pattern to that of Ni₂P. The situation is different for the sample Ni-P/SiO₂ (Ni:P = 2:1) (Figure 2(c)). In this case, the Ni-P peak was reduced to a shoulder and the Ni-Ni peak shifts to the metallic position. It is evident that this sample is different from Ni₂P. For the Ni-P/SiO₂ (Ni:P = 3:1), the two Fourier transform peaks were merged into one, and a broad peak appears at a shorter bond distance (Figure 2(d)). Clearly, in this case, there is disruption from the Ni₂P structure.

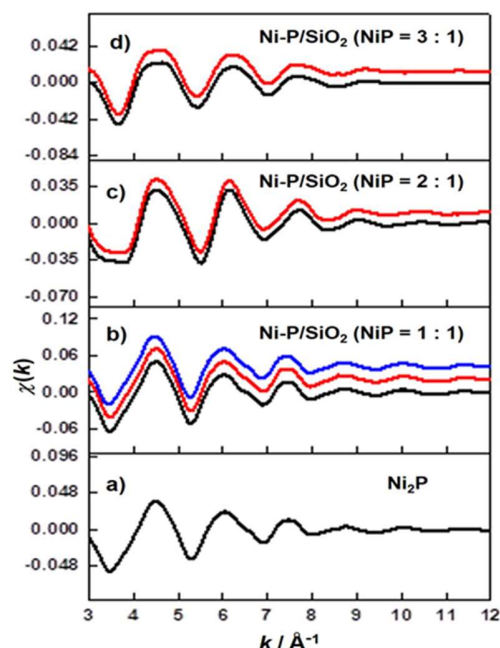


Figure 1. Comparison of nickel K-edge EXAFS spectrum: a) bulk Ni₂P, b) Ni-P/SiO₂ (Ni:P = 1:1), c) Ni-P/SiO₂ (Ni:P = 2:1), d) Ni-P/SiO₂ (Ni:P = 3:1). The reaction times for the Ni-P/SiO₂ samples are 0 h (black), 3 h (red), and 12 h (blue).

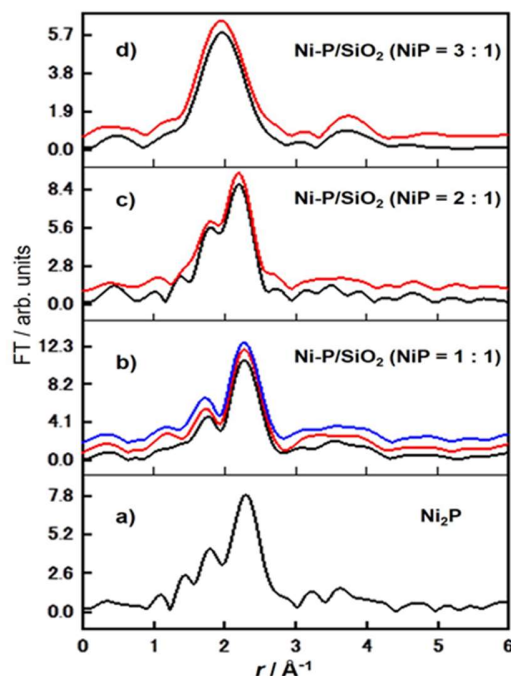


Figure 2. Comparison of Ni K-edge EXAFS oscillation results Fourier transforms: a) reference Ni₂P, b) Ni-P/SiO₂ (Ni:P = 1:1), c) Ni-P/SiO₂ (Ni:P = 2:1), d) Ni-P/SiO₂ (Ni:P = 3:1). The reaction times for the Ni-P/SiO₂ samples are 0 h (black), 3 h (red), and 12 h (blue).

Table 1. Curve fitting results of the Ni K-edge EXAFS spectra for the Ni₂P reference and different samples with initial Ni:P ratios of 1:1, 2:1, and 3:1.

Samples	Ni-Ni				Ni-P				R% ^c
	CN ^a	R (Å) ^b	σ (Å) ^c	ΔE (eV) ^d	CN ^a	R (Å) ^b	σ (Å) ^c	ΔE (eV) ^d	
Fresh samples									
Ni ₂ P reference	4.0±0.3	2.62±0.02	0.092	5.4	1.0±0.3	2.21±0.02	0.071	-5.1	0.5
Ni-P (1:1, 0h)	4.6±0.6	2.62±0.02	0.085	3.4	1.3±0.3	2.19±0.02	0.081	-7.5	0.3
Ni-P (2:1, 0h)	4.2±0.3	2.52±0.02	0.093	-1.1	0.6±0.3	2.18±0.03	0.036	-7.3	0.1
Ni-P (3:1, 0h)	4.6±0.9	2.45±0.02	0.116	-7.2	2.0±0.5	2.28±0.02	0.139	-3.6	0.5
Spent samples									
Ni-P (1:1, 3h)	4.5±0.8	2.62±0.03	0.082	3.5	1.5±0.5	2.18±0.03	0.084	-9.8	0.5
Ni-P (2:1, 3h)	4.3±0.3	2.53±0.03	0.095	-0.7	0.7±0.3	2.17±0.03	0.058	-8.8	0.3
Ni-P (3:1, 3h)	4.6±1.0	2.46±0.02	0.117	-6.6	2.1±0.6	2.28±0.03	0.131	-2.3	0.4

^a Coordination numbers.

^b Interatomic distance.

^c Debye-Waller factor.

^d Edge shift.

^e Residual factor.

Table 1 shows the curve fitting analysis of the peaks in Figure 2. The curve fitting analysis was conducted for EXAFS oscillations [$\chi(k) \cdot k^3$] in the k space obtained by backscattering Fourier transform filtered FT spectra. The curve fitting analysis indicated the Ni-P and Ni-Ni bond distances were 2.19 Å and 2.62 Å, respectively, for Ni-P/SiO₂ (Ni:P = 1:1). These bond distances agree well with those found in Ni₂P reference within the error bar. In the case of Ni-P/SiO₂ (Ni:P = 2:1), the curve fitting analyses indicated the Ni-Ni bond distance was 2.52 Å while that of Ni-P was 2.18 Å. But the Ni-Ni and Ni-P distances were 2.45 Å, and 2.28 Å observed in Ni-P/SiO₂ (Ni:P = 3:1) from the curve fitting analysis. The Ni-Ni bond distance was shorter than that of Ni metal. So, the NOCM catalytic activity was high due to the presence of the Ni₂P phase, and it was stable during non-oxidative coupling of methane (NOCM) reactions at 1173 K. Still, the other two samples were less active in catalytic reaction might be the absence of Ni₂P structure. It is interesting and important to make the relation between activity and structure to know the reason for fewer activities of initial Ni:P ratios of 2:1 and 3:1 and to design another new type of Ni-P/SiO₂ catalysts. But it is not easy to determine the nickel phosphide phase only by the EXAFS CF method.

X-ray absorption near-edge structure (XANES) is a powerful technique for investigating the local structure of inorganic-oxide-supported catalysts, which is more sensitive to the electronic states and 3-dimensional geometric structures than EXAFS spectroscopy. Due to the lack of experimental reference compounds, I carried out XANES and EXAFS calculations based on the model structures using FEFF8. Theoretical XAFS calculations using the FEFF program have enabled us to reproduce the XAFS spectra in both the XANES and EXAFS regions.^{4,5} I attempted to analyze the structure of

Ni phosphide catalysts by comparing with the theoretical XAFS spectra of reference compounds based on their crystal structures instead of by comparing with experimental XAFS spectra of analyzing compounds. Figure 3 shows the FEFF-calculated theoretical XANES spectra of NiP₃, NiP₂, NiP, Ni₅P₄, Ni₂P, Ni₁₂P₅, and Ni₃P. For the peak positions comparison of experimental and theoretical XANES spectra, I extracted peak positions in XANES spectra.

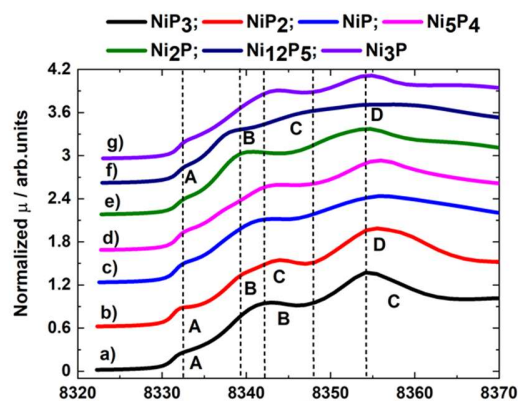


Figure 3. Comparison of Ni K-edge theoretical XANES spectra of reference compounds: a) FEFF NiP₃ (black line), b) FEFF NiP₂ (red line), c) FEFF NiP (blue line), d) FEFF Ni₂P (pink line), e) FEFF Ni₅P₄ (green line), f) FEFF Ni₁₂P₅ (navy line), and g) FEFF Ni₃P (violet line).

Figure 4 shows the comparison of Ni K-edge XANES, inversely Fourier Transform (IFT) and Fourier transform (FT) of the Ni_2P reference sample with the FEFF8 calculated theoretical spectra. The experimental and theoretical XANES spectra of Ni_2P show the same three features (labeled A, B, and C). To estimate the systematic error, I compared the peak positions in the experimental and calculated Ni_2P spectra. The differences between the experimental and calculated peak energies were 0.0, -0.4, and 0.0 eV for features A, B, and C, respectively (Table 2).

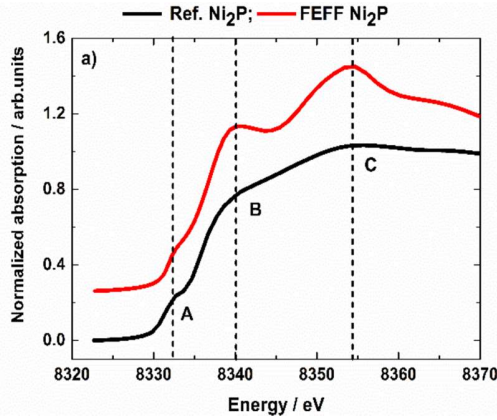


Figure 4. Comparison of experimental and theoretical Ni K-edge XANES spectra of Ni_2P .

Table 2. Experimental and theoretical peak positions in XANES spectra of Ni_2P .

Ref. Ni_2P (eV)	FEFF8 Ni_2P (eV)	ΔE (eV)
8332.7	8332.7	0.0
8339.7	8340.1	-0.4
8354.7	8354.7	0.0

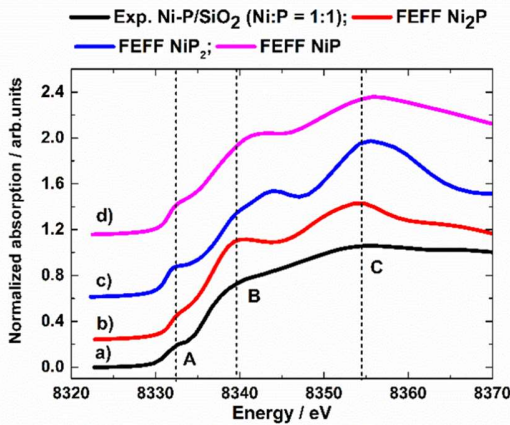


Figure 5. Comparison of Ni K-edge XANES spectra for a) Ni-P/SiO_2 ($\text{Ni:P} = 1:1$) (black), b) FEFF Ni_2P (red), c) FEFF NiP_2 (blue), and d) FEFF NiP (pink).

Figure 5 shows the Ni K-edge XANES spectrum of Ni-P/SiO_2 ($\text{Ni:P} = 1:1$), together with those of Ni_2P , NiP_2 , and NiP calculated using FEFF8. The experimental XANES spectrum of Ni-P/SiO_2 ($\text{Ni:P} = 1:1$) shows three main peaks (A, B, and C). The Ni K-edge peak pattern in the theoretical XANES spectrum of the reference Ni_2P compound agrees with the experimental spectrum of Ni-P/SiO_2 ($\text{Ni:P} = 1:1$). Peaks A, B, and C in their theoretical XANES spectrum appeared at positions corresponding to Ni-P/SiO_2 ($\text{Ni:P} = 1:1$): 8332.7, 8339.7, and 8354.7 eV. The theoretical XANES spectra of the other reference compounds show peaks at different positions. These results suggest that Ni-P/SiO_2 ($\text{Ni:P} = 1:1$) predominantly had the Ni_2P structure. These results agreed with our previous CF results.

We calculated the EXAFS oscillation on the basis of the Ni_2P crystal structure and compared the spectrum with that of the Ni-P/SiO_2 ($\text{Ni:P} = 1:1$) catalyst in k -spaces as shown in Figures 6. We found good agreement between the experimental and calculated spectra. In this analysis, we used an S_0^2 of 0.9 and σ^2 values of 0.009 and 0.0095 \AA^2 for Ni-P and Ni-Ni bonds, respectively. By theoretical approaches, we concluded that the Ni-P/SiO_2 ($\text{Ni:P} = 1:1$) consisted mainly of the Ni_2P structure. We applied the same methods to the other Ni phosphide catalysts.

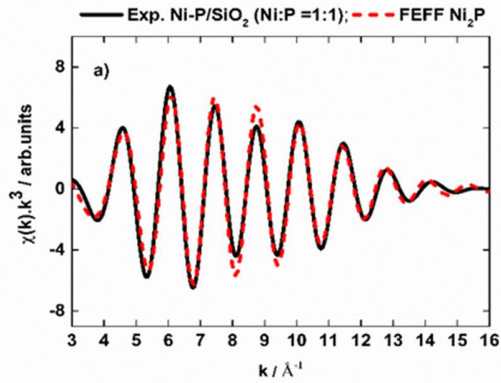


Figure 6. Comparison between theoretical Ni_2P (red broken line) and experimental EXAFS spectra of Ni-P/SiO_2 ($\text{Ni:P} = 1:1$) (black line).

Figure 7 shows a comparison of the experimental and theoretical XANES spectra of Ni-P/SiO_2 ($\text{Ni:P} = 2:1$). Four peaks (A, B, C, and D) appear in the spectra. The experimental spectrum agrees well with the theoretical Ni K-edge XANES spectrum of Ni_{12}P_5 . For this composition, the energy differences between the experimental and theoretical peak positions are all within ± 0.4 eV. The theoretical XANES spectra for other compositions show larger deviations in peak positions from the experimental spectrum. Consequently, we concluded that the experimental spectrum was consistent with the phase Ni_{12}P_5 .

I then calculated the EXAFS spectrum on the basis of the Ni_{12}P_5 crystal structure. Figure 8 compares the experimental EXAFS spectrum of Ni-P/SiO_2 ($\text{Ni:P} = 2:1$) with the theoretical spectrum of Ni_{12}P_5 . The fitting corresponds well with each other. The S_0^2 factors for Ni-P and Ni-Ni were both fixed at 0.9, and the σ^2 factors were fixed at 0.007 and 0.0075 \AA^2 , respectively.

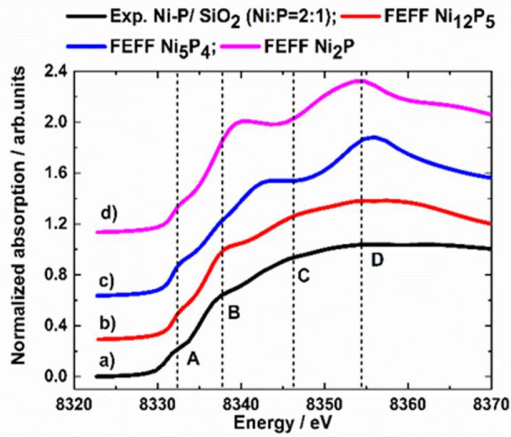


Figure 7. Comparison of Ni K-edge XANES spectra: a) Ni-P/SiO₂ (Ni:P = 2:1) (black line), b) FEFF Ni₁₂P₅ (red line), c) FEFF Ni₅P₄ (blue line), and d) FEFF Ni₂P (pink line).

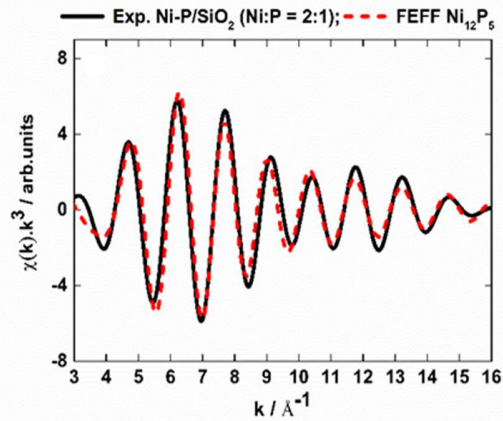


Figure 8. Comparison between theoretical Ni₁₂P₅ (red broken line) and experimental Ni-P/SiO₂ (Ni:P = 2:1) (black line) EXAFS spectra.

Figure 9 shows a comparison of the experimental XANES spectrum of Ni-P/SiO₂ (Ni:P = 3:1) and the calculated spectra of three Ni-rich reference compounds. The XANES structure was immensely broad in the experimental data. I observed three peaks (A, B, and C) in the spectrum of Ni-P/SiO₂ (Ni:P = 3:1). The peak positions corresponded well with the peak positions in the theoretical Ni₃P spectrum. I simulated theoretical EXAFS spectra on the basis of the Ni₃P crystal structure. The S_0^2 and σ^2 values for Ni-P and Ni-Ni were set at 0.9 and 0.009 Å², respectively. Figure 10 shows the theoretical EXAFS spectra for the Ni₃P structure, the experimental EXAFS spectra for Ni-P/SiO₂ (Ni:P = 3:1), and their corresponding FTs. We found that the calculated EXAFS data successfully reproduced the experimental data. In particular, we observed a single peak in the FT of the Ni-P/SiO₂ (Ni:P = 3:1) spectrum and the Ni₃P spectrum (Figure 10 (b)). Thus, we confirmed the formation of the Ni₃P phase in Ni-P/SiO₂ catalysts with an initial Ni:P ratio of 3:1.

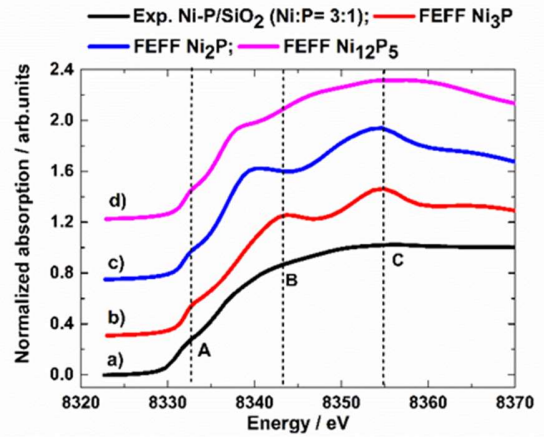


Figure 9. Comparison of Ni K-edge XANES spectra: a) Ni-P/SiO₂ (Ni:P = 3:1) (black line), b) Ni₃P FEFF (red line), c) Ni₂P FEFF (blue line), and d) Ni₁₂P₅ FEFF (pink line).

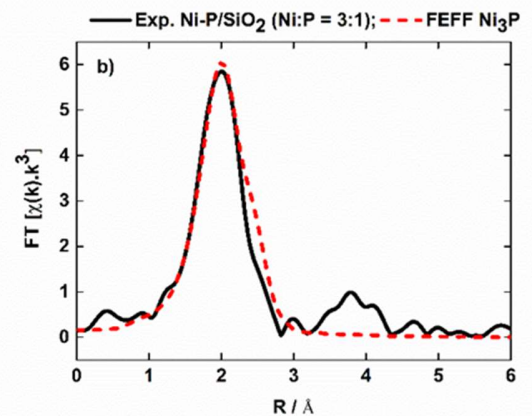
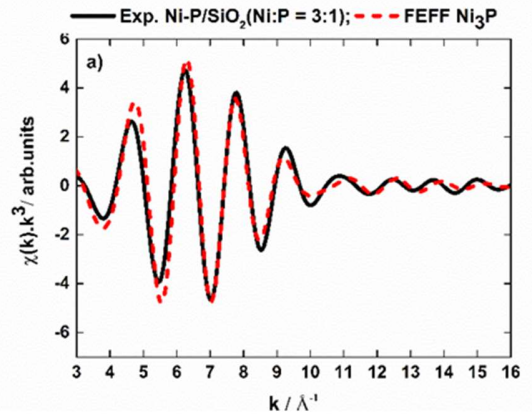


Figure 10. a) Comparison between theoretical Ni₃P (red broken line) and experimental (black line) EXAFS spectra of Ni-P/SiO₂ (Ni:P = 3:1) (black line); b) corresponding Fourier transforms.

In these analyses, I only used the theoretical reference XANES and EXAFS spectra calculated by FEFF. By comparing the experimental and theoretical XANES data for Ni_2P , we observed that the experimental XANES peaks were broadened, and thus I concentrated on the peak position energy. I found that, even if the structures of Ni phosphide compounds were complicated, I could predict an unknown structure by comparing the experimental data with the theoretical XANES and EXAFS data without recording the spectra of the corresponding reference compounds experimentally. The structures of Ni-P/SiO₂ with Ni:P ratios of 1:1, 2:1, and 3:1 were identified as Ni_2P , Ni_{12}P_5 , and Ni_3P , respectively, on the basis of theoretical FEFF calculations of their XANES and EXAFS spectra. In the case of Ni-P/SiO₂ samples with Ni:P = 1:1 and Ni:P = 2:1, the Ni:P ratio in the precursor was greater than the Ni:P ratios in the resultant Ni_2P and Ni_{12}P_5 because, during the preparation processes under reductive conditions at high temperature, P was volatilized as PH_3 . Additional P atoms were, therefore, necessary and were supplied by the reduction of coexisting PO_4 .⁶ Ni_2P lost more P than Ni_{12}P_5 , and Ni_{12}P_5 lost substantially more P than Ni_3P . The presence of more Ni might have prevented the loss of P from the sample due to the Ni adsorption ability, which decreases with the increase of P.⁷

In the case of NOCM reactions, Ni-P/SiO₂ (Ni:P = 1:1) exhibited the highest catalytic performance among the investigated Ni phosphide catalysts. The Ni-P/SiO₂ (Ni:P = 1:1) structure corresponded to Ni_2P . More Ni-rich phosphide compounds such as Ni_{12}P_5 and Ni_3P exhibited lower activity. Pure metallic Ni efficiently activated the C–H bond in CH_4 and decomposed the CH_4 to coke, which poisoned and deactivated the Ni surface. In the crystal structure of Ni_2P , the shortest Ni–Ni bond length is 2.61 Å (Table 3). In Ni_{12}P_5 and Ni_3P , the shortest Ni–Ni bond lengths are 2.53 Å and 2.44 Å, respectively. These shorter bond lengths might have led to the higher activity for C–H bond cleavage in CH_4 and the formation of coke that suppressed the catalytic activity. A higher P content increases the Ni–Ni bond length, which decreases Ni activity. Thus, an appropriate Ni:P ratio provides a good balance between CH_4 activity and preventing coke formation during NOCM reactions. The Ni_2P /SiO₂ catalyst had a suitable Ni:P balance that activated the large amount of methane to methyl radical than the Ni_{12}P_5 /SiO₂ and Ni_3P /SiO₂ and consequently form ethane, ethylene, benzene and so on.¹

Table 3. Nickel-Nickel bond distances of various nickel phosphide catalysts.

Compound Name	$R_{\text{Ni-Ni}}$ (Shortest) ^{CF,a} (Å)	$R_{\text{Ni-Ni}}$ (Shortest) ^{The,*b} (Å)
Ni_2P	2.62±0.02	2.61
Ni_{12}P_5	2.52±0.02	2.53
Ni_3P	2.45±0.02	2.44

^a Al Rashid et al., 2020⁸; ^b Ren et al., 2007⁹

In the previous theoretical analysis, I showed that FEFF could predict the unknown structure for Ni phosphide complex systems with some systematic error. FEFF can successfully reproduce the peaks features in the XANES spectra for the Ni_2P complex system (Figure 4). But due to the difference in peak shape in FEFF calculated XANES spectra at B, I observed that the peak position difference is -0.4 eV. Since FPMS is a different approach that used non-muffin tin approximation where the potential is assumed to be anisotropic in each atomic sphere, and the interstitial region contains charge density, I expect quietly good results in the Ni_2P complex system to overcome the peak shape problem. In this case, the FPMS method has been applied in the Ni_2P complex system for XANES calculations and compared between FPMS (NMT) calculated XANES spectra with FEFF (MT) calculated XANES spectra. I have tested the present full potential multiple scattering (FPMS) schemes for X-ray absorption near edge structure (XANES) calculations of the Ni_2P complex system.

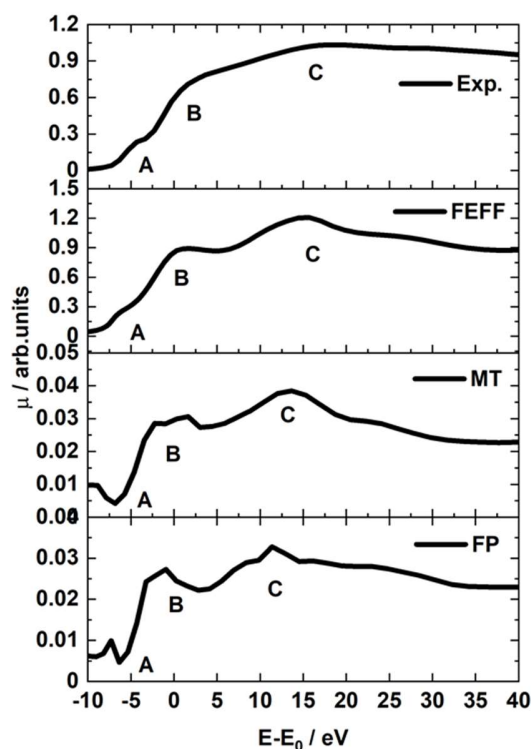


Figure 11. Comparison of Ni K-edge XANES spectra in the experimental, FEFF, Muffin-tin (MT, Prof. K. Hatada coding), and Full potential (FP) analyzing results.

Figure 11 shows the comparison of Ni K-edge XANES spectra of Ni_2P for the Prof. K. Hatada coding muffin-tin (MT), full potential (FP), FEFF, and experimental analyzing results. In the MT and FP calculated XANES spectra, I found that pre-edge peak A and the oscillatory features between peak B and C. For FP calculated XANES spectra, the peak features were sharper than the MT calculated XANES spectra. On the other, the experimental and FEFF calculated XANES spectra of Ni_2P had significant A, B, and C peak features that were different

from the MT and FP peak features. The FP calculated XANES spectra had only a vague pre-edge peak position compare to the FEFF. In contrast, B and C peak features were zigzag types in FPMS calculated XANES spectra. But FEFF calculated XANES spectra given clear B and C peak features that agreed well with experimental Ni₂P XANES spectra. Figure 11 (b) XANES spectra was calculated by the FPMS executive file where the full potential parameter was “MT” in the input file. This spectrum should be the same as FEFF calculated XANES spectra (Figure 11 (c)), because both potentials were calculated using muffin-tin approximation. But in this case, the peak features of MT (Prof. K. Hatada coding) did not correspond with FEFF. This result was indicating some of the parameters in the data.ms input file did not work well.

FPMS is a brand new method for XANES calculations. For the first time, I have tried to apply this method for XANES calculation in the Ni phosphide complex system. This analyzing result was not expecting. During the calculations of XANES spectra using FPMS, I faced some problems during the XANES calculations using FPMS: 1) FPMS is a time-consuming program than the FEFF. It takes a long run time to execute the FPMS data file. 2) Peak resolution determination is one of the serious problems for FPMS analysis. 3) Radius of scattering site and empty cell determination is also difficult for the FPMS calculations. Due to the lack of a user guide in English, I cannot execute the input file properly. I need to adjust some parameters to get the good XANES spectra using FPMS. I will continue the FPMS analysis; after that, I can expect high-quality XANES spectra for Ni₂P using the FPMS method.

Conclusion

In this thesis, I have successfully revealed the local structure of silica-supported Ni phosphide with different Ni:P ratios by X-ray absorption fine structure (XAFS) and determined the unknown structure for non-oxidative coupling of methane (NOCM) reactions. I have shown that the XAFS analysis is powerful to unveil the structure of the complex system, which is sensitive to the local structure of the supported metal catalysts and is usually used to determine the structure. The conventional curve fitting results demonstrated that Ni-P/SiO₂ with initial Ni:P ratio 1:1 had a Ni₂P phase for NOCM reaction. Interestingly, the schematic mol ratio of Ni:P is 1:1, where the formation mol ratio of Ni:P was 2:1 for Ni₂P structure. More P had been used to prepare the Ni₂P structure because some of the P is evaporated under reduction or ultra vacuum conditions. Less P induces the phase transition to Ni₁₂P₅ or the other phase. This result is indicating the excess P to modify the properties of nickel phosphide catalyst.

The theoretical FEFF method has been used for the calculation of reference spectra used as pattern fitting. The pattern fitting results of XANES spectra confirmed that the Ni:P ratio of the 1:1 sample generated Ni₂P, which ensured the EXAFS CF results, where Ni₁₂P₅ and Ni₃P phases were introduced with the change Ni:P ratios as 2:1 and 3:1 respectively. The theoretical EXAFS data were also simulated to compared with the experimental EXAFS data using the theoretical FEFF method. This approach was different from the CF method. The theoretical EXAFS data were successfully

reproduced the experimental EXAFS data. It was ensured that the theoretical model which produced the experimental data well could predict the unknown complex structure.

I observed the effect of the Ni:P ratio on the structure and activity of the catalysts. The suitable amount of Ni:P ratio controls the NOCM catalytic activity. Since Ni₂P is the most active phase for NOCM reactions than the other two, so Ni₂P/SiO₂ had the best balance of Ni:P ratio. Another important parameter, Ni-Ni bond distance, played an important role in catalytic activity. In the Ni₂P structure, the shortest Ni-Ni bond distance is 2.61 Å, where the shortest bond distance of Ni₁₂P₅ and Ni₃P are 2.53 Å and 2.44 Å, respectively. These results demonstrated that the moderate bond lengths of Ni-Ni balanced the C-H bond cleavage in CH₄ and the formation of coke that suppressed the catalytic activity.

Another brand new theoretical method full potential multiple scattering (FPMS) were used to calculate the XANES. This method is different from the conventional FEFF method. This method based on the absorption signal calculated in the FP approximation sometimes proves excellent fits to the experimental spectra. However, I expected a better result from this new theoretical approach. But unfortunately, the results were not satisfying.

In summary, the XAFS method can determine the local structure around metal and provide us quantitative and qualitative information. Furthermore, the theoretical approach determines the unknown complex structures without experimental reference. I have revealed that Ni₂P is the most active phase for methane conversion reactions. Moreover, I have established a relation between structure and catalytic structure in this thesis, which is important for developing the new active Ni phosphide catalyst. I hope this thesis has made an epoch for the XAFS analysis in this new century.

Reference

- 1 A. L. Dipu, S. Ohbuchi, Y. Nishikawa, S. Iguchi, H. Ogihara, I. Yamanaka, *ACS Catal.* **2020**, *10*, 375.
- 2 K. Asakura, ed. by Yasuhiro Iwasawa, World Scientific, **1996**, Vol. 58, pp. 33–58.
- 3 S. I. Zabinsky, J. J. Rehr, A. Ankudinov, R. C. Albers, M. J. Eller, *Phys. Rev. B* **1995**, *52*, 2995.
- 4 J. J. Rehr, R. C. Albers, *Rev. Mod. Phys.* **2000**, *72*, 621.
- 5 E. Bosman, J. Thieme, *J. Phys. Conf. Ser.* **2009**, *186*.
- 6 K. K. Bando, Y. Koike, T. Kawai, G. Tateno, S. T. Oyama, Y. Inada, M. Nomura, K. Asakura, *J. Phys. Chem. C* **2011**, *115*, 7466.
- 7 M. Kiskinova, D. W. Goodman, *Surf. Sci.* **1981**, *108*, 64.
- 8 M. H. Al Rashid, A. Dipu, Y. Nishikawa, H. Ogihara, Y. Inami, S. Obuchi, I. Yamanaka, S. Nagamatsu, D. Kido, K. Asakura, *e-Journal Surf. Sci. Nanotechnol.* **2020**, *18*, 24.
- 9 J. REN, J. guo WANG, J. fen LI, Y. wang LI, *Ranliao Huaxue Xuebao/Journal Fuel Chem. Technol.* **2007**, *35*, 458.